Soils and Rocks
An International Journal of Geotechnical and Geoenvironmental Engineering
www.soilsandrocks.com
ISSN 1980-9743
ISSN-e 2675-5475

Influence of T-bar test penetration rate on undrained shear strength of a laboratory clayey mixture

Daniel de Andrade Faria[1], Vinícius Batista Godoy[2#], Fernando Schnaid[3], Lucas Festugato[3]

Technical Note

Keywords
Undrained shear strength
T-bar penetrometer
Clayey soil
Penetration rate

Abstract

Extensive and accurate data from on-site testing is increasingly fundamental in determining design geotechnical parameters of offshore structures. As a novel method for assessing offshore soil, the T-bar penetrometer offers benefits such as high precision, reliability, ample data acquisition and cost-effectiveness, but its application in offshore projects remains limited. In this research, a set of approaches are used to analyze the evaluation of penetration rate effects in a kaolin and bentonite mixture prepared to reproduce Brazilian offshore soil conditions aiming the development of in situ testing technology in the marine engineering area. Miniature T-bar penetrometer tests (10 mm diameter and 50 mm length) at constant driving penetration rate were performed at 0.05; 0.1; 0.25; 0.5; 1.0; 2.5 and 5.0 mm/s. In addition, three variable rate tests (twitch tests) were performed aiming to analyze the penetration rate reductions at each twitch stage. The measured resistances and the drainage conditions were interpreted using the normalized velocity (V), and the results show a strength increase by viscous effects of 10% for each logarithmic cycle of penetration rate increase. The results suggest that the transition between the undrained and partially drained penetration occurs at normalized penetration rates between 20 and 50. These results agree with values previously published in the literature and unequivocally demonstrate how the influence of penetration rate can impact the measured undrained shear strength for T-bar tests. It is concluded that the influence of the test penetration rate on the measured resistance cannot be disregarded in intermediate permeability soils.

1. Introduction

The development and expansion of offshore activities (e.g. cross-sea bridges, offshore oil and gas drilling platforms, offshore wind energy, tidal energy power generation, submarine tunnels and offshore mineral extraction) put forward higher requirements on the sensitivity, safety, and durability of geotechnical engineering, especially on the evaluation of the performance of offshore structures under loading effects and related design parameters (Qiao et al., 2023).

The planning and building of offshore structures require extensive and accurate data (Guo et al., 2015, 2021; Qiao et al., 2023). Thus, on-site testing is increasingly fundamental in determining design parameters. As a novel method for assessing offshore soft soil, the T-bar penetrometer offers benefits such as high precision, reliability, ample data acquisition and cost-effectiveness. Nevertheless, while utilized in onshore engineering, its application in offshore projects remains limited (Cai et al., 2021; Qiao et al., 2023).

In this scenario, the study of loading penetration rate effects is of great importance for the interpretation of undrained shear strength in clay and silty soils obtained as demonstrated by both field and laboratory tests (e.g. Randolph, 2004; Almeida et al., 2011; Jannuzzi et al., 2012; Schnaid et al., 2020). It is widely recognized that the measured resistance increases with the reduction of penetration rate due to the occurrence of partial drainage around the probe whereas with increasing penetration rate an increase in resistance is observed due to the predominance of viscous effects (e.g. Lehane et al., 2009; Graham et al., 1983; Fisher & Cathie, 2003; Einav & Randolph, 2005).

In the case of marine clay deposits, full-flow penetrometers such as T-bar and Ball are broadly used for the investigation of undrained strength. According to Randolph (2004) these instruments have projected area 5 to 10 times greater than the cross-sectional area of the driving shaft, which improves the accuracy in estimate of shear strength profiles in soft soils. International standards and recommendations (e.g.

[#]Corresponding author. E-mail address: vinigodoy@msn.com
[1]Klohn Crippen Berger, Porto Alegre, RS, Brasil.
[2]Analysis Consultoria, Porto Alegre, RS, Brasil.
[3]Universidade Federal do Rio Grande do Sul, Programa de Pós-Graduação em Engenharia Civil, Porto Alegre, RS, Brasil.

Submitted on October 23, 2023; Final Acceptance on September 12, 2024; Discussion open until May 31, 2025.
Editor: Renato P. Cunha
https://doi.org/10.28927/SR.2025.010423

ISO, 2023) use as reference a monotonic penetration rate of 20 ± 5 mm/s.

The degree of consolidation during the penetration test is controlled by the normalized velocity (V), defined by Finnie & Randolph (1994) as:

$$V = \frac{vD}{c_v} \tag{1}$$

where v is the penetration rate, D is the diameter of the penetrometer and c_v is the soil consolidation coefficient. According to Randolph & Hope (2004), in piezocone tests (CPTu) penetration is considered fully drained for normalized velocity (V) below 0.1 and undrained for values above 10. Within this range, partial drainage conditions prevail.

For relatively low-test rates, the penetrometers resistance decreases with increasing loading rate, being controlled by drainage conditions. However, when penetration rate is high, soil viscous effects become significant and penetration resistance typically increases by 5 to 20% per logarithmic cycle increase in strain rate (Graham et al., 1983; Einav & Randolph, 2005). According to Randolph (2004), this increase can be expressed as:

$$Su = Su_{ref}\left[1 + \mu log\left(\frac{\dot{\gamma}}{\dot{\gamma}_{ref}}\right)\right] \tag{2}$$

where $\dot{\gamma}$ is the shear strain rate, Su_{ref} is a reference strength, measured at a reference shear strain rate ($\dot{\gamma}_{ref}$), and μ is the strain rate coefficient, which reflects the percentage increase in strength per logarithmic cycle. For the T-bar penetrometer, numerical simulations by Zhou & Randolph (2009) suggest that the average strain rate around the penetrometer is approximately $v/(3D)$. Alternatively, when analysing a specific case with defined geometry, normalized velocities (V) or driving velocities (v) can be used in Equation 2 instead of strain rates.

The semi-logarithmic fit (Equation 2) has the disadvantage of not representing the decrease in the influence of viscous effects at low penetration rates (or strain rates). For this purpose, an alternative type of fit can be used, which is based on the hyperbolic arc sine function:

$$\frac{Su}{Su_{ref}} or \frac{q}{q_{ref}} = 1 + \frac{\mu}{\ln(10)}\left[arsinh\left(\frac{V}{V_0}\right) - arsinh\left(\frac{V_{ref}}{V_0}\right)\right] \tag{3}$$

where q is the penetration resistance and V_0 is a normalized penetration rate below which the influence of viscous effects begins to reduce.

In this research, this set of equations and approaches (Graham et al., 1983; Einav & Randolph, 2005; Qiao et al., 2023) are used to analyze the evaluation of penetration rate effects in a clay mixture prepared to reproduce Brazilian offshore soil conditions aiming the development of in situ testing technology in the marine engineering area.

2. Materials

With the purpose of reproducing, in the laboratory, the behavior of marine clayey soils, several studies applied mixtures of kaolin (100%) or kaolin with bentonite in varying proportions (Lourenço et al., 2020; O'Loughlin et al., 2020; Sampa et al., 2021). The production of artificial soil allows for better homogeneity, workability and geotechnical parameters control for laboratory analysis.

The clayey material used in this research consists of a laboratory-produced mixture composed of 85% kaolin and 15% bentonite (by dry weight) and a moisture content of 120%. This mixture presents high plasticity, good workability and geotechnical characteristics similar to those of Brazilian marine clays (Petrobras, 2011).

For mixture preparation, initially dry materials were hand mixed for better homogenization. The amount of water added to obtain a moisture content of 120% was corrected considering the natural moisture content of the materials. Then, the materials were blended in a mixer with an effective capacity of 100 L and mechanically homogenized.

Specific Gravity of Soil Solids tests were performed according to ASTM D854 (ASTM, 2014) and for particle-size analysis ASTM D422 – 63 (ASTM, 2007) guidelines were applied. For the material passing through the 2 mm sieve, Granulometry by Sedimentation and Fine Sieving was performed. It is worth mentioning that for the analysed samples there was no material retained in this sieve, that is, no coarse sieving was performed.

Table 1 shows the results of the geotechnical characterization tests of the kaolin, bentonite and the mixture composed of 85% kaolin and 15% bentonite, with a moisture content of 120%.

According to ASTM D2487 (ASTM, 2017), the kaolin, bentonite and the mixture are classified as CH (High Plasticity Clay). Based on the Activity Index (A_i) kaolin is classified as an inactive clay, and the percentage of 15% of bentonite added to the mixture is sufficient to make it an active clay, with a colloidal activity index (A_i) of 1.6.

The grain size distribution of the studied materials, obtained by sedimentation, is shown in Figure 1. At the end of the tests, the material was poured into a 0.075 mm sieve, however the amount of retained material was negligible.

Figure 1 also shows that the gain size distribution of the mixture is very similar to the ones of marine clays from the Santos Basin - Brazil (Petrobras, 2011), especially for grain diameters smaller than 0.03 mm. Field clayey soils present, on average, 25 to 60% clay, 35 to 60% silt and 5 to 15% sand. In addition, the liquid limit of 103%, the plasticity limit of 37% and the plasticity index of 66% are also remarkably close to the average values obtained at depths of up to 10 m in the Santos Basin (Brazil) – LL = 100%, PL = 40% and

Table 1. Geotechnical characterization of kaolin, bentonite and mixture.

	Kaolin	Bentonite	Mixture
Natural Moisture Content - *h* (%)	1.4	16.5	3.6
Specific Gravity of Soil Solids - G_s (g/cm^3)	2.594	2.645	2.602
Liquid Limit – *LL* (%)	43	448	103
Plastic Limit – *PL* (%)	29	90	37
Plasticity Index – *PI* (%)	14	358	66
% Clay (*Ø* ≤ 0.002 mm)	32	81	40
% Silt (0.002mm < *Ø* ≤ 0.06 mm)	67	19	60
% Sand (0.06mm < *Ø* ≤ 2 mm)	1	0	1
Colloidal activity index - *Ai*	0.44	4.41	1.60

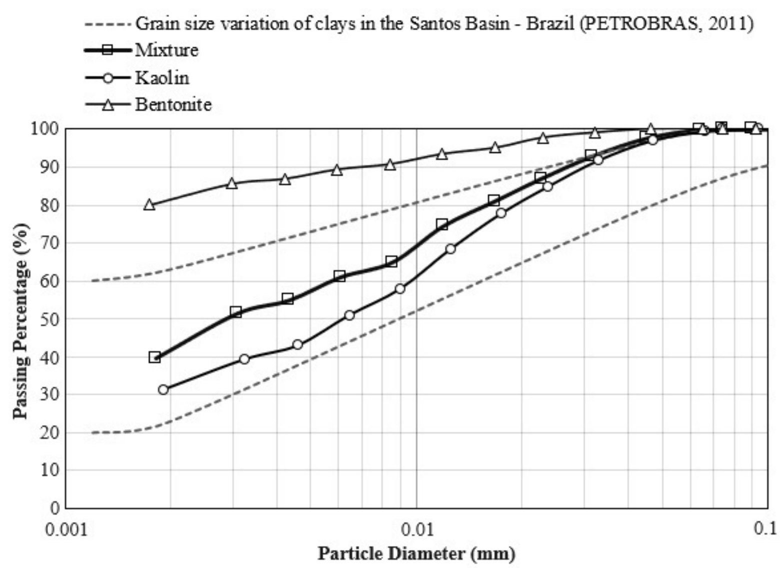

Figure 1. Grain size distribution of the analysed mixture, kaolin and bentonite.

PI = 60%, approximately (Petrobras, 2011). Therefore, it can be concluded that the geotechnical characteristics of the clayey mixture used are similar to those of the Brazilian marine clayey soils taken as reference.

3. Analysis and results

One-dimensional consolidation tests were carried out following the guidelines of ASTM D2435 (ASTM, 2011) and ASTM D4186 (ASTM, 2012). Molds in the form of stainless-steel rings with an internal diameter of 5 cm and a height of 2 cm were used. At the beginning of the test, filter paper and porous stones were saturated, the loading apparatus was balanced, and a linear displacement transducer (LVDT) and an analogic displacement gauge were installed to determine specimens' height variation.

The test started with the application of a 2.32 kPa preload (for 5 minutes), including the contribution of LVDT, porous stone, and top-cap. After this period, the initial reading (zero reference) was defined. Each stage of the test, both unloading and loading, lasted at least 24 hours and the unloading stages occurred with at least three stages.

Table 2 presents the initial and final conditions of the four specimens tested, where h_0 and h_f are the initial and final moisture contents of the sample, e_0 is the initial void ratio, ρ_{hi} and ρ_{hf} are the initial and final specific mass, and S_0 and S_f are the initial and final saturation degrees.

Figure 2 presents the void ratio curves (*e*) as a function of vertical stress (σ_v) obtained for the samples tested. In the AM1 and AM2 tests, the first point is below the initial void ratio of the samples because of the settling preload of 2.32 kPa generated by the top cap weight. Despite these minor differences in the initial sections, all tests converged to the same compression line.

In this research, Taylor's (1942) methodology was applied to determine the consolidation coefficient (c_v). This method is based on the curve's shape of the consolidation percentage versus the square root of the time factor. From the beginning of primary consolidation, a straight line was drawn with abscissa equal to 1.15 times the corresponding

Table 2. Initial and final characteristics of the tested specimens – Consolidation Tests.

Sample	h_0 (%)	ρ_{hi} (g/cm³)	e_0	S_0 (%)	h_f (%)	ρ_{hf} (g/cm³)	S_f (%)
AM1	116.3	1.371	3.12	96.96	55.98	1.653	99.43
AM2	116.3	1.377	3.11	97.49	56.83	1.657	100.00
AM3	118.4	1.366	3.20	97.22	66.53	1.570	97.81
AM4	118.3	1.373	3.18	97.80	68.12	1.599	100.00

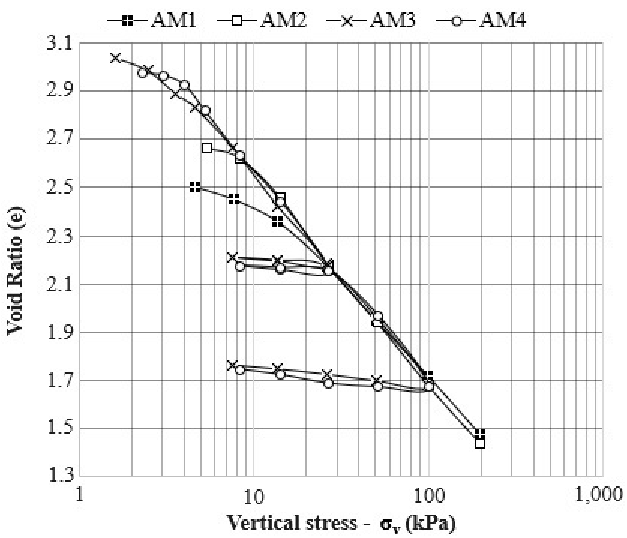

Figure 2. Void ratio (e) as a function of vertical stress (σ_v) – Consolidation Tests.

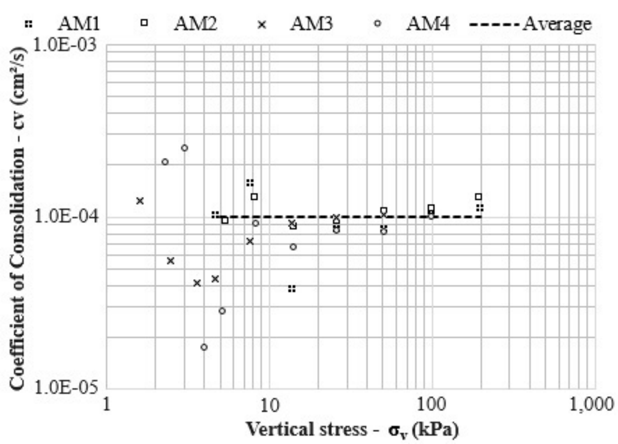

Figure 3. Coefficient of consolidation (cv) as a function of vertical stress (σ_v) – Consolidation Tests.

abscissa of the initial straight line. The intersection of this line with the test curve indicates the point at which 90% of the settlements would have occurred. Having defined the time corresponding to 90% settlement (t_{90}) the consolidation coefficient can then be determined using Equation 4:

Table 3. Parameters obtained in the consolidation tests.

Sample	Compression Index (C_c)	Expansion Index (C_s)	c_v average (cm²/s)
AM1	0.7963	-	9.86 x 10^{-5}
AM2	0.8883	-	1.07 x 10^{-4}
AM3	0.8139	0.0794	7.89 x 10^{-5}
AM4	0.9090	0.0926	1.02 x 10^{-4}
Average	0.8519	0.0860	9.66 x 10^{-5}

$$c_v = \frac{0,848\, H_d^{\,2}}{t_{90}} \tag{4}$$

where H_d is half the average height of the specimen and the t_{90} is the time at which 90% of the settlements would have occurred. The coefficient of consolidation (c_v) obtained for each loading stage is shown in Figure 3.

It is possible to notice that the consolidation coefficient tends to an average value of approximately 1.00 x 10^{-4} cm²/s for vertical stresses above 5 kPa, as indicated by the dashed line in Figure 3. For lower stresses, the small variations in the sample height reduce the representativity of the determination of this parameter, with significant variability. The coefficients determined with the AM3 and AM4 samples showed a small tendency to increase with the reduction in vertical stresses (σ_v).

Table 3 presents the compressibility parameters and the average consolidation coefficient obtained for each test. The expansion indexes obtained corresponded to approximately one tenth of the compression indexes ($C_s/C_c \approx 0.1$).

The miniature 10 mm and a length of 50 mm T-bar cylinder used in the research was made of stainless steel (projected area of 500 mm²). The driving rod had a diameter of 8 mm, with a projected area of 50.3 mm², corresponding to approximately 10% of the projected area of the T-bar cylinder, as shown in Figure 4.

The penetration and extraction of the penetrometer in the soil were carried out using a set formed by a stepper motor with programmable driver, in addition to a gearbox, a ball screw, guide rods and a sliding platform with vertical movement, where the rod is fixed. This setup can be seen in Figure 5. The motor is activated using software that allows programming the predefined driving rate, displacement and direction, as well as the number of steps per revolution

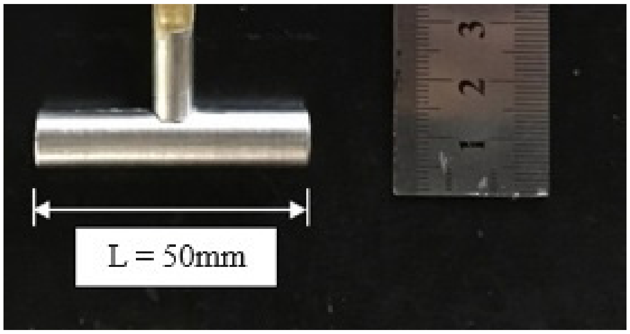

Figure 4. T-bar penetrometer used.

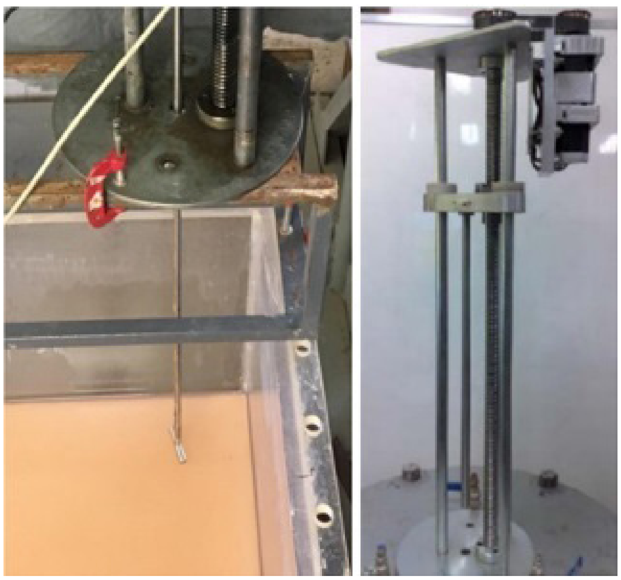

Figure 5. Penetrometer driving system.

of the motor. The penetration resistance during the tests was measured through a S-type load cell, with a capacity of 100 kgf, positioned between the sliding platform of the driving system and the penetrometer rod.

A reference driving rate (v_{ref}) of 2.5 mm/s (equivalent to $0.25D_{T\text{-}bar}$) was adopted as recommended by Lunne et al. (2011). The lowest penetration rate was 0.025 mm/s, corresponding to one hundredth of the reference penetration rate.

Tests at constant driving penetration rate were performed at 0.05; 0.1; 0.25; 0.5; 1.0; 2.5 and 5.0 mm/s. Three tests were performed with rates of 0.5, 1.0 and 2.5 mm/s, and two tests with each of the other rates.

In addition to the constant-penetration rate tests, three variable rate tests (twitch tests) were performed. The procedure usually employed in these tests is to reduce the penetration rate by half at each stage. However, to cover a wider range, and considering that the investigation depth was limited, a greater penetration rate reduction was selected at each stage. Table 4 presents the penetration stages used in the tests performed.

Table 4. Driving penetration rates employed at each stage of the Twitch trials.

Stage	Depth (cm)	Driving rate (mm/s)
1	0-8	2.5
2	8-10	1.0
3	10-12	0.5
4	12-14	0.25
5	14-16	0.1
6	16-18	0.05
7	18-20	0.025
8	20-28	2.5

Figure 6 shows a comparison of the twitch TW1 test and the constant penetration rate T-bar test results in the same tank but in different locations avoiding superposition of effects. The points corresponding to driving rate reductions performed and the consequent differences in measured resistance between the standard and the twitch test are clearly illustrated in Figure 6. After returning to the standard driving penetration rate, at the last transition point, the twitch test curve undergoes a considerable increase, reaching a resistance practically equal to that of the standard test, which shows that results can be properly compared and correlated. Figure 7 shows the TW2 and TW3 tests, along with the reference tests.

Figure 8a shows the resistance ratio (q/q_{ref}) expressed as a function of a test penetration rate determined by both twitch tests and tests with constant rates (different from the standard). The studies by Finnie & Randolph (1994) and O'Loughlin et al. (2020) indicated that the consolidation of the analyzed soil has a high influence on the resistance values measured in penetration tests. In that regard, Figure 8b presents the values of resistance ratio as a function of the normalized velocities calculated using the average coefficient of consolidation (c_v) determined from the consolidation tests.

For test normalization, the reference penetration rate (*vref*) was 2.5 mm/s, as adopted by Randolph (2004) and Lunne et al. (2011) in previous publications. The measured resistance ratios were adjusted according to the functions expressed in Equations 2 and 3. In the inverse hyperbolic sine function fit (Equation 3), the penetration rate $v0$ was set as 0.125 mm/s as recommended by the above authors, because it corresponds to the value at which the influence of viscous effects begins to reduce.

Values of q_t/q_{ref} are relatively constant for lower penetration rates, between 0.025 and 0.05 mm/s, and within this range both viscous and partial drainage effects appear to be negligible. The determined μ coefficient was 0.1, which represents a 10% increase in resistance at each logarithmic cycle (10-fold increase) in penetration rate. This value is within the range commonly described by similar studies (e.g. Einav & Randolph, 2005), ranging from 5% to 20%.

Data in Figure 8b, suggests that the transition between the undrained and partially drained penetration occurs at

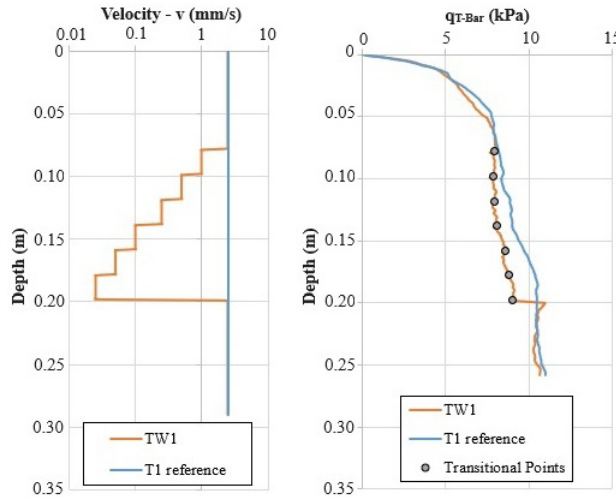

Figure 6. Comparison between standard penetration rate T-bar test and Twitch TW1 test.

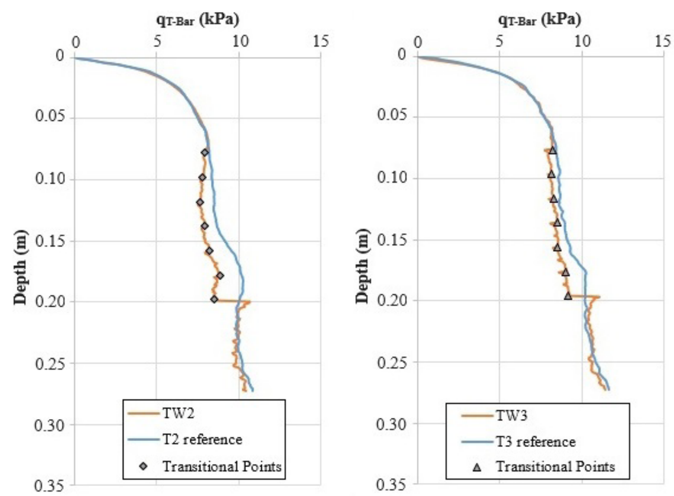

Figure 7. Twitch TW2 and TW3 tests with the respective reference tests.

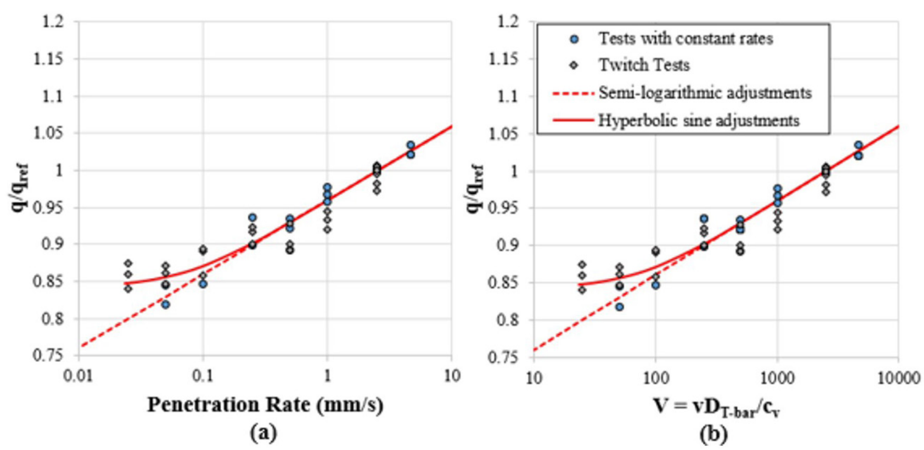

Figure 8. Resistance ratios as a function of (a) test penetration rate and of (b) normalized velocity, with semi-logarithmic and hyperbolic sine adjustments.

normalized penetration rates between 20 and 50, which agrees with the values typically reported (between 10 and 30).

These results agree with values previously published in the literature and unequivocally demonstrate how the influence of penetration rate can impact the measured undrained shear strength for T-bar tests. It is concluded that the influence of the test penetration rate on the measured resistance, cannot be disregarded in intermediate permeability soils.

4. Conclusion

This research analyzed the evaluation of the penetration rate effects in a clay mixture prepared to reproduce Brazilian offshore soil conditions with a view to developing in situ testing technology in the marine engineering area. The use of the T-bar penetrometer indicated accuracy, reliability, and extensive data acquisition.

Besides that, the present work evaluates the rate increase in undrained shear strength predicted from T-bar penetrometer tests performed at various penetration rates in a clay mixture produced in the laboratory. Variations in strength are expressed as a function of both penetration rate and normalized velocity to define a backbone curve for T-bar penetration conceived to capture partial drainage effects and viscous effects. The results adjusted by a hyperbolic sine curve and a semi-logarithmic function indicate a resistance increase of 10% with each penetration rate increase in logarithmic cycle due to viscous effects. Partial drainage effects are perceived for normalized velocities lower than $V = 25$. These results agree with values previously published in the literature and unequivocally demonstrate how the influence of penetration rate can impact the measured undrained shear strength for tests such as the T-bar.

In recent years, T-bar penetrometer technology has been applied in many countries in North America and Europe. However, the use of this field test is not yet widespread, especially in South America. In this sense, it is still necessary to carry out a large number of field tests to verify the applicability of the T-bar penetrometer in offshore soils of South America.

Acknowledgements

The authors wish to express their appreciation to the Brazilian Oil Company Petrobras [grant number: 3.20.1903(306)], as well the Brazilian National Council for Technology Development – (CNPq) - (grant number: 141338/2019-9) for technical and financial support.

Declaration of interest

The authors have no conflicts of interest to declare. All co-authors have observed and affirmed the contents of the paper and there is no financial interest to report.

Authors' contributions

Daniel de Andrade Faria: conceptualization, methodology, data curation, investigation. Vinícius Batista Godoy: conceptualization, writing - original draft. Fernando Schnaid: conceptualization, methodology, supervision, validation. Lucas Festugato: conceptualization, methodology, supervision, validation.

Data availability

All data produced or examined in the course of the current study are included in this article.

Declaration of use of generative artificial intelligence

This work was prepared without the assistance of any generative artificial intelligence (GenAI) tools or services. All aspects of the manuscript were developed solely by the authors, who take full responsibility for the content of this publication.

List of symbols and abbreviations

c_v	coefficient of consolidation
e	void ratio
h	moisture content
q	penetration resistance
t_{90}	time at which 90% of the settlements would have occurred
u	pore pressure
v	loading penetration rate
Ai	colloidal activity index
C_c	compression index
CH	high plasticity clays
C_s	expansion index
D	diameter of the penetrometer
G_s	specific gravity of soil solids
H_d	half the average height of the specimen
LL	liquid limit
LVDT	linear displacement transducer
PI	plasticity index
PL	plastic limit
S	saturation degree
Su	undrained shear strength
V	normalized velocity
V_0	normalized penetration rate below which the influence of viscous effects begins to reduce
$\dot{\gamma}_{ref}$	reference shear strain rate
μ	strain rate coefficient
ρ_s	specific mass
σ'_v	effective vertical stress
$Ø$	diameter

References

Almeida, M.S.S., Oliveira, J.R.M.S., Motta, H.P.G., Almeida, M.C.F., & Borges, R.G. (2011). CPT and T-bar penetrometers for site investigation in centrifuge tests. *Soils and Rocks*, *34*(1), 79-88. http://doi.org/10.28927/SR.341079.

ASTM D422-63. (2007). *Standard Test Method for Particle-Size Analysis of Soils*. ASTM International, West Conshohocken, PA. https://doi.org/10.1520/D0422-63R07.

ASTM D2435. (2011). *Standard Test Methods for One-Dimensional Consolidation Properties of Soils Using Incremental Loading*. ASTM International, West Conshohocken, PA. https://doi.org/10.1520/D2435-04.

ASTM D4186. (2012). *Standard Test Method for One-Dimensional Consolidation Properties of Saturated Cohesive Soils Using Controlled-Strain Loading*. ASTM International, West Conshohocken, PA. https://doi.org/10.1520/D4186-06.

ASTM D854. (2014). *Standard Test Methods for Specific Gravity of Soil Solids by Water Pycnometer*. ASTM International, West Conshohocken, PA. https://doi.org/10.1520/D0854-23.

ASTM D2487. (2017). *Standard Practice for Classification of Soils for Engineering Purposes (Unified Soil Classification System)*. ASTM International, West Conshohocken, PA. https://doi.org/10.1520/D2487-17.

Cai, G., Liu, S., Peng, P., & Yang, Y. (2021). *Theory and engineering application of marine in situ testing technology*. Science Press of Beijing.

Einav, I., & Randolph, M.F. (2005). Combining upper bound and strain path methods for evaluating penetration resistance. *International Journal for Numerical Methods in Engineering*, *63*(14), 1991-2016. http://doi.org/10.1002/nme.1350.

Finnie, I.M.S., & Randolph, M.F. (1994). Punch-through and liquefaction induced failure of shallow foundations on calcareous sediments. In *Proceedings of 7th International Conference on Behaviour of Offshore Structures* (Vol. 1, pp. 217-230). Cambridge, Massachusetts: Pergamon.

Fisher, R., & Cathie, D. (2003). Optimisation of gravity based design for subsea applications. In *Proceedings of BGA International Conference On Foundations* (pp. 283-296). Dundee, London: Thomas Telford Limited. https://doi.org/10.1680/fiodap.32446.0027.

Graham, J., Crooks, J.H.A., & Bell, A.L. (1983). Time effects on the stress-strain behaviour of natural soft clays. *Geotechnique*, *33*(3), 327-340. http://doi.org/10.1680/geot.1983.33.3.327.

Guo, Z., Hong, Y., & Jeng, D.S. (2021). Structure–seabed interactions in marine environments. *Journal of Marine Science and Engineering*, 9(9), 972. http://doi.org/10.3390/jmse9090972.

Guo, Z., Yu, L., Wang, L., Bhattacharya, S., Nikitas, G., & Xing, Y. (2015). Model tests on the long-term dynamic performance of offshore wind turbines founded on monopiles in sand. *Journal of Offshore Mechanics and Arctic Engineering*, *137*(4), 041902. http://doi.org/10.1115/1.4030682.

ISO 19901-8. (2023). *Petroleum and natural gas industries. Specific requirements for offshore structures. Part 8: Marine soil investigations*. International Organization for Standardization, Geneva.

Jannuzzi, G.M.F., Danziger, F.A.B., & Martins, I.S.M. (2012). Cyclic T-Bar Tests to evaluate the remoulded undrained shear strength of the Sarapuí II Soft Clay. *Soils and Rocks*, *35*(3), 279-294. http://doi.org/10.28927/SR.353279.

Lehane, B.M., O'louglin, C.D., Gaudin, C., & Randolph, M.F. (2009). Rate ffects on penetrometer resistance in kaolin. *Geotechnique*, *59*(1), 41-52. http://doi.org/10.1680/geot.2007.00072.

Lourenço, D., Schnaid, F., & Schettini, E.B.C. (2020). Model pile installation by vertical water jet in clay. *Journal of Offshore Mechanics and Arctic Engineering-Transactions of the ASME*, *142*(4), 045001. http://doi.org/10.1115/1.4046169.

Lunne, T., Andersen, K.H., Low, H.E., Randolph, M.F., & Sjursen, M. (2011). Guidelines for offshore in situ testing and interpretation in deepwater soft clays. *Canadian Geotechnical Journal*, *48*(4), 543-556. http://doi.org/10.1139/t10-088.

O'Loughlin, C.D., Zhou, Z., Stanier, S.A., & White, D.J. (2020). Load-controlled cyclic T-bar tests: a new method to assess effects of cyclic loading and consolidation. *Géotechnique Letters*, *10*(1), 7-15. http://doi.org/10.1680/jgele.19.00030.

Petrobras. (2011). *Internal report. 0-11*. Petrobras.

Qiao, H., Liu, L., He, H., Liu, X., Liu, X., & Peng, P. (2023). The practice and development of T-Bar penetrometer tests in offshore engineering investigation: a comprehensive review. *Journal of Marine Science and Engineering*, *11*(6), 1160. http://doi.org/10.3390/jmse11061160.

Randolph, M.F. (2004). Characterisation of soft sediments for offshore applications. In *Proceedings of the 2nd International Conference on Site Characterization (ISC)* (Vol. 1, pp. 209-232). Rotterdam: Millpress.

Randolph, M.F., & Hope, S. (2004). Effect of cone velocity on cone resistance and excess pore pressures. In *Proceedings of the International Symposium on Engineering Practice and Performance of Soft Deposits* (pp. 147-152). Osaka: Japanese Geotechnical Society.

Sampa, N.C., Schnaid, F., Rocha, M.M., Cudmani, R., & Amaral, C.S. (2021). Vertical and horizontal pullout capacity of mooring lines embedded in very soft clays. *Ocean Engineering*, *234*, 109229. http://doi.org/10.1016/j.oceaneng.2021.109229.

Schnaid, F., Dienstmann, G., Odebrecht, E., & Maghous, S. (2020). A simplified approach to normalization of

piezocone penetration rate effects. *Geotechnique*, *70*(7), 1-25. http://doi.org/10.1680/jgeot.18.T.033.
Taylor, D.W. (1942). *Research on consolidation of clays*. Massachusetts Institute of Technology.
Zhou, H., & Randolph, M.F. (2009). Resistance of full-flow penetrometers in rate dependent and strain-softening clay. *Geotechnique*, *59*(2), 79-86. http://doi.org/10.1680/geot.2007.00164.